

EXPANSION OF COARSE-GRAINED FLUIDIZED BEDS
 IMPEDED BY HORIZONTAL TUBE ARRAYS

V. A. Borodulya, V. V. Matsnev,
 Yu. G. Epanov, Yu. S. Teplitskii,
 and B. I. Gorelik

UDC 66.096.5

Experimental data on the expansion of fluidized beds with immersed arrays of horizontal tubes are obtained and generalized.

The practical utilization of a promising solid-fuel processing technique - low-temperature burning in a fluidized-bed boiler assembly - is attracting considerable attention in power engineering at the present time. In furnace equipment of this type 50-70% of the heat released in burning of the fuel is withdrawn from the bed by means of heat exchangers, which are generally made in the form of horizontal or slightly inclined arrays of tubes immersed partially or completely in the fluidized bed. The expansion of the bed in the tube array determines the working zone and efficiency of the furnace and is therefore a necessary characteristic for the analysis and design of heat exchangers for the fluidized-bed furnace units of power-generating boilers.

Limited information on this topic is available in the literature and is concerned mainly with porosity measurements in beds of finely dispersed [1, 2] and coarsely dispersed [3] materials. The correlation proposed in [4] for calculating the expansion of a bed containing a tube array involves parameters that are difficult to determine, in particular the rate of ascent of gas bubbles, and is poorly suited to engineering calculations.

The objective of the present study is to determine the fundamental laws governing the expansion of fluidized beds impeded by tube arrays and to formulate generalized correlations for calculating the working height of the bed.

The experiments were carried out on two arrangements with different tube array configurations. The first arrangement (K.1) comprised a metal column of rectangular cross section 40 x 25 cm and height 1.5 m. The forward wall was made of clear plastic for visual observation of the bed. A packet of horizontal tubes of outside diameter 20 or 30 mm arranged in a checkerboard or straight-line (corridor) pattern was placed in the column at various heights from the gas distributor. The packet occupied the entire horizontal cross section of the fluidized-bed apparatus. The second arrangement (K.2) represented a one-tenth scale model of the fully installed E/pr-420-140KS fluidized-bed boiler assembly [the model was installed in the experimental station of the Scientific-Industrial Union (NPO) of the I. I. Polzunov Central Scientific-Research Institute for Boilers and Turbines (TsKTI)]; it had plan dimensions

TABLE 1. Characteristics of the Experimental Materials

Bed material	d, mm	ρ_s , kg/ m ³	ϵ_0	u_0 , m/ sec	Notation in text
Aluminum silicate catalyst	4	1300	0,4	1,14	M.1
Crumbled fireclay	3	2300	0,48	0,95	M.2
Glass balls	1,7	2600	0,4	0,65	M.3
Peas	6	1300	0,4	1,4	M.4
Pearl barley	3	1200	0,42	0,75	M.5
Millet	2	1100	0,39	0,55	M.6

A. V. Lykov Institute of Heat and Mass Transfer, Academy of Sciences of the Belorussian SSR, Minsk. Scientific-Industrial Union of the I. I. Polzunov Central Scientific-Research Institute for Boilers and Turbines, Leningrad. Translated from *Inzhenerno-Fizicheskii Zhurnal*, Vol. 54, No. 6, pp. 989-994, June, 1988. Original article submitted August 26, 1986.

TABLE 2. Experimental Conditions for Investigation of the Expansion of Fluidized Beds In Horizontal Tube Bundles

Tube configuration in array	$S_H \times S_V$, mm	D, mm	Bed material	H_0 , cm	H_T , cm	h , cm	u , m/sec	Remarks
Checkerboard	100×100	30	M.3, M.4, M.5	30, 52, 76, 41, 31, 56, 30	160	0	0.7-2.4	K.1. Bed completely impeded by tube array
Checkerboard	80×80	20, 30	M.3	37	160	0	0.8-2.3	
Checkerboard	60×60	30	M.2, M.3, M.4, M.5, M.6	39, 25, 52, 75, 37, 39, 37	160	0	0.6-2.4	
Checkerboard	45×45	30	M.2, M.3, M.6	25		0	0.5-1.4	
Corridor	60×60	30	M.5, M.6	30, 62, 30	160	0	0.6-2.0	
Corridor	60×60	30	M.3	25, 36, 50, 13, 30, 41, 49, 61, 13, 23, 36, 26, 39	27 41 75 75	0 17 14 26	0.8-2.0 0.7-1.9 0.8-2.0 0.8-2.0	K.1. Bed partially impeded by tube array
Checkerboard	40×18	10	M.1	10, 13, 18	16	7.2	1.8-3.8	K.2. Bed partially impeded by tube array

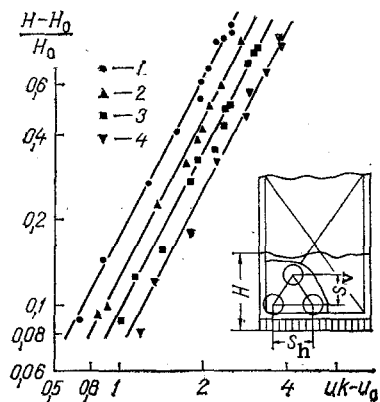


Fig. 1

Fig. 1. Influence of tube array geometry on the expansion of a fluidized bed completely impeded by a tube array in arrangement K.1: material M.3 ($uk - u_0$, m/sec). 1) $S_h \times S_v = 100 \times 100$ mm; 2) 80×80 mm; 3) 60×60 mm; 4) 45×45 mm.

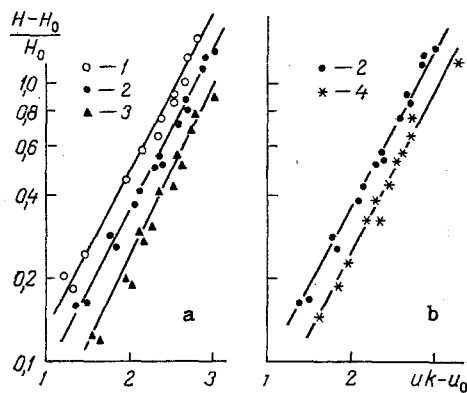


Fig. 2

Fig. 2. Influence of the size (a) and density (b) of the particles of disperse material on the expansion of a fluidized bed completely impeded by a tube array, $S_h \times S_v = 60 \times 60$ mm. 1) M.6; 2) M.5; 3) M.4; 4) M.2.

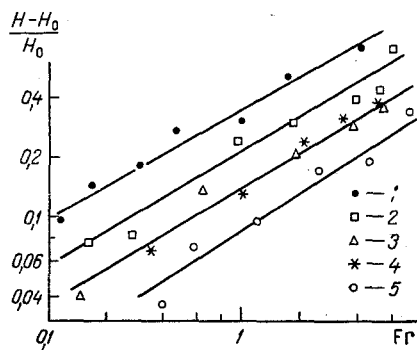


Fig. 3

Fig. 3. Expansion of a fluidized bed completely impeded by a tube array vs Fr for material M.3 and tubes arranged in a straight-line pattern with spacing $S_h \times S_v = 60 \times 60$ mm, $h = 17$ cm, $H_t = 41$ cm. 1) Bed completely impeded by tube; 2) $H_0 = 30$ cm; 3) 41 cm; 4) 49 cm; 5) unimpeded bed.

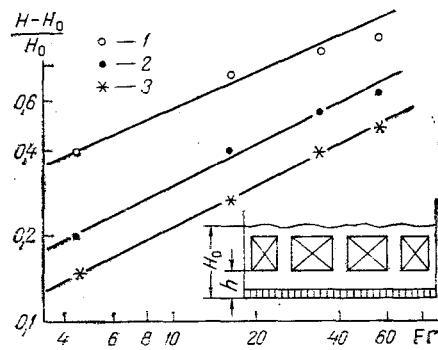


Fig. 4

Fig. 4. Relative expansion $(H - H_0)/H_0$ vs Fr in arrangement K.2. 1) $H_0 = 10$ cm; 2) 13 cm; 3) 18 cm.

of 83×26 cm and was fabricated entirely of clear plastic. The tube array consisted of four separate tube packets of diameter 10 mm separated by corridors of width 60 mm (see Fig. 4). The tubes in the array were arranged in a checkerboard pattern with six vertically tiered rows, and the bottom row of tubes was placed at a distance of 72 mm from the gas distributor. Provision was made for the insertion of tubes into the corridors during the experiments. Perforated gas distributors were installed in both columns. The characteristics of the narrow-fraction disperse materials are given in Table 1, and the experimental conditions are summarized in Table 2. The coolant was air at room temperature. The expansion of the bed was determined visually from the position of the upper boundary of the bed. The error of measurement of the relative expansion did not exceed 15%.

Figure 1 shows typical results characterizing the influence of the tube array geometry on the relative expansion of a fluidized bed totally impeded by a tube array in arrangement K.1. The appreciable influence of the tube spacing on the expansion of the bed, which also depends significantly on the excess air filtration rate, is evident from the figure. In the investigated range of filtration rates $(H - H_0)/H_0$ is proportional to the quantity $(uk - u_0)$ raised to a power close to 2. It has been proposed [5-7] that this fact be exploited to control the load of steam generators with a fluidized-bed furnace unit. The dependence of the

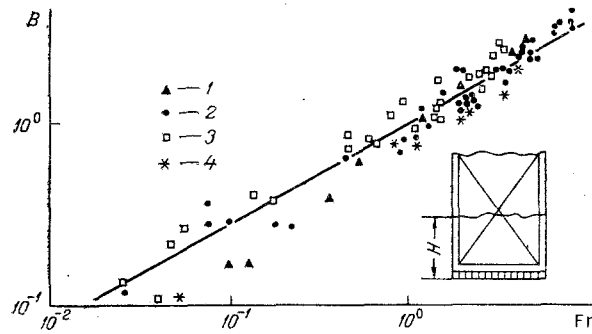


Fig. 5. Generalization of experimental data on the expansion of a fluidized bed completely impeded by a tube array. 1) $S_h \times S_v = 45 \times 45$ mm; 2) 60×60 mm; 3) 80×80 mm; 4) 100×100 mm.

$$B = \frac{((H - H_0)/H_0) (\rho_s/\rho_f)^{0,21}}{0,82 ((S_h - D)/d)^{0,26}}$$

relative expansion of the bed on the diameter and density of the particles is shown in Fig. 2. It is important to note the experimentally disclosed independence of the expansion from the as-filled height of the fluidized bed, which evinces the stabilizing action of the arrays on the size and velocity of the gas bubbles.

The placement of the tube array in the middle section of the fluidized bed with free-bed zones above and below the array causes the expansion of the bed to decrease (Fig. 3). It is evident from this figure that the expansion of the bed for any arrangement of a tube packet in its middle zone is always greater than in the free (unimpeded) bed ($H_t = 0$) and is always smaller than in the bed completely impeded by a tube array ($h = 0$, $H_t \geq H_0$).

It is also important to note the distinctive attributes of the expansion process when the as-filled height of the bed is varied. As H_0 is increased in the interval $h < H_0 < H_t$, the relative expansion of the bed decreases. The value of H_0 is not observed to have any appreciable influence on the expansion for $H_0 > H_t$ (Fig. 3).

The results of the experiments on arrangement K.2 are shown in Fig. 4. It was observed that the expansion does not depend on the presence or absence of corridors between the individual tube packets in the array. This is evidently attributable to the insignificant fraction of corridors (at most 25%) in the total volume of the tube-filled bed.

An analysis of the experimental data on the influence of the parameters of the bed and the tube array on the expansion of a fluidized bed completely filled with a horizontal array of tubes enables us to determine the form of the functional relation used to generalize the results. The following empirical correlation was obtained by multivariate-regression and correlation analysis on a computer:

$$\frac{H - H_0}{H_0} = 0.82 Fr^{0,55} \left(\frac{\rho_s}{\rho_f} \right)^{-0,21} \left(\frac{S_h - D}{d} \right)^{0,26} \quad (1)$$

The results of more than 200 experiments described by Eq. (1) with an rms scatter of 22% are generalized in Fig. 5. It follows from the functional relation (1), which is derived on the basis of experiments at room temperature, that $(H - H_0)/H_0$ decreases as the air temperature is increased (and, accordingly, as the gas density ρ_f is decreased). Unfortunately, the literature does not provide any data on the expansion of a tube-impeded fluidized bed at elevated temperatures. Our own estimates on the basis of Eq. (1) show that $(H - H_0)/H_0 = 0.95$ at $T_{fb} = 20^\circ\text{C}$ in a bed of coarsely dispersed material (crumbled fireclay, $d = 3$ mm), but at $T_{fb} = 900^\circ\text{C}$ the relative expansion decreases to 0.7 for a constant excess filtration rate.

This behavior of the expansion with increasing temperature of the bed is qualitatively consistent with observations made in the combustion of a gas in an unimpeded bed [8] and also with the analysis of these experiments in [9].

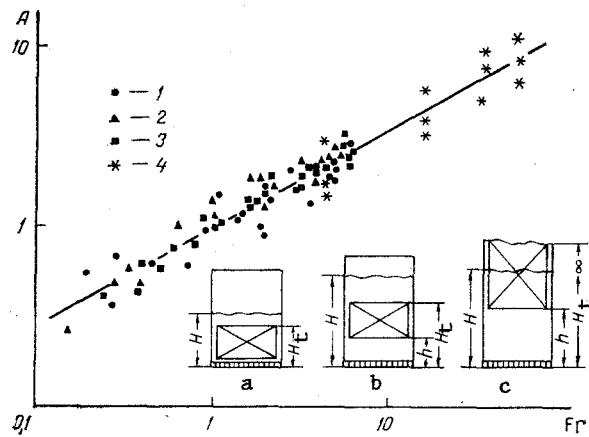


Fig. 6. Generalization of experiments on the expansion of a fluidized bed partially impeded by a tube array:

$$A = \left(\frac{H - H_0}{H_0} \right) / \left[0.82 \left(\frac{\rho_s}{\rho_f} \right)^{-0.21} \left(\frac{S_h - D}{d} \right)^{0.26} - 0.165 \left(\frac{H_0}{H_t - h} \right)^{0.3} \right]$$

- 1) Tube array in position a; 2) in position b; 3) in position c; 4) in position b (TsKTI experiments).

In practice the tube array is usually placed at a certain height h from the gas-distributing grid. In this case, as we mentioned above, the expansion of the bed is smaller than in the bed completely filled with tubes, and it depends on the relation between the parameters H_t , h , and H_0 . Taking Eq. (1) as our basis and assuming that the influence of the tube-free zones of the bed is characterized by the generalized group $H_0/(H_t - h)$ formed from the geometrical parameters of the bed and the tube array, we generalize the experimental data by the correlation

$$\frac{H - H_0}{H_0} = 0.82 Fr^{0.55} \left(\frac{\rho_s}{\rho_f} \right)^{-0.21} \left(\frac{S_h - D}{d} \right)^{0.26} - 0.165 Fr^{0.55} \left(\frac{H_0}{H_t - h} \right)^{0.3}, \quad (2)$$

in which the second term reflects the influence of the unimpeded bed above and below the tube array on the net expansion of the bed. It should be noted that the second term vanishes formally as $h \rightarrow 0$ and $H_t \rightarrow \infty$ (case of expansion only in the tube array), and the functional relation (2) goes over to Eq. (1). Thus, the expansion of the fluidized bed with a tube array immersed in it is determined not only by the array geometry, but also by its position within the volume of the bed (Fig. 6).

The above-established relations (1) and (2) are valid in the following ranges of the parameters: $0.1 \leq Fr \leq 60$; $900 < \rho_s/\rho_f < 2200$; $2.5 \leq (S_h - D)/d \leq 46.6$; $0.2 < H_0/(H_t - h) < 2.5$; they can be used for calculations of the expansion of fluidized beds with immersed horizontal tube arrays.

NOTATION

d , D , diameters of particles in bed and tubes in array; h , placement height of tube array above gas-distributing grid; H , H_0 , height of fluidized bed in working state and as-filled height of bed; H_t , distance from gas distributor to axial line of top row of tubes in array; k , porosity of tube array; S_h , S_v , horizontal and vertical spacings of tubes in array; u , u_0 , gas filtration rate and fluidization startup rate; ε_0 , porosity of bed at minimum fluidization; T , temperature; ρ , density; $Fr = (uk - u_0)^2/gS_v$. Indices: fb, fluidized bed; f, gas; s, solid particles.

LITERATURE CITED

1. N. I. Gel'perin, V. G. Ainshtein, and N. A. Romanova, *Khim. Prom.*, No. 11, 1-8 (1962).

2. N. I. Gel'perin, V. G. Ainshtein, and A. V. Zaikovskii, *Khim. Neft. Mashinostr.*, No. 3, 17-20 (1968).
3. V. N. Korolev and N. I. Syromyatnikov, *Inzh.-Fiz. Zh.*, 37, No. 5, 829-835 (1980).
4. A. M. Xavier and J. F. Davidson, in: *Proc. Second Engineering Foundation Conference*, Cambridge Univ. Press, London-New York (1978), pp. 333-336.
5. Yu. G. Epanov, A. I. Tamarin, and S. S. Zabrodskii, *Fuel Combustion with Minimum Harmful Flare-Ups* [in Russian], Tallin (1978), pp. 13-14.
6. V. V. Matsnev, I. N. Shteiner, and B. I. Gorelik, *Teploénergetika*, No. 4, 10-13 (1983).
7. B. I. Gorelik, "Improvement of the operational reliability and efficiency of solid-fuel combustion in furnaces with a low-temperature fluidized bed," *Authors's Abstract of Candidate's Dissertation, Engineering Sciences, Leningrad* (1986).
8. N. V. Antonishin and S. S. Zabrodskii, *Inzh.-Fiz. Zh.*, 5, No. 2, 10-14 (1962).
9. S. S. Zabrodskii, *High-Temperature Fluidized-Bed Apparatus* [in Russian], Moscow (1971).

MODELING THERMAL REGIMES OF OBJECTIVES

IN OPTOELECTRONIC DEVICES

G. N. Dul'nev, V. V. Barantsev,
and V. G. Parfenov

UDC 536.24

A numerical method is proposed for calculating the temperature field of objectives in optoelectronic devices, based on use of the stage-by-stage modeling method. A set of programs realizing the technique are described.

The thermal regime of optoelectronic devices has a significant effect on the quality and reliability of their operation. An important part of the mathematical modeling of such a device used for design purposes is modeling of the thermal regime. An optoelectronic device is a complex system, including varied optical, mechanical, and electronic components.

The basic method for designing complex systems is the block-hierarchical method, in which the system is successively considered at different hierarchy levels with a gradually increasing degree of detail. The stage-by-stage method of mathematical modeling of heat transport processes, the general principles of which are presented in [1], is most satisfactory for the block-hierarchical method. A hierarchy of component levels for optoelectronic devices for thermal modeling purposes was proposed in [2], with four levels of detail being distinguished. On the first level we have individual elements: mirrors, lenses, reflectors, etc.; on the second level we have optical, mechanical, and electronic devices: lasers, objectives, servolines, etc.; on the third, optoelectronic devices; and on the fourth, groups of devices located in one compartment or one chassis. Such a level structure agrees with the hierarchy of optoelectronic device description used in designing such devices [3].

An essential feature of modeling heat exchange processes is the necessity of considering a process of one and the same physical nature for the entire optoelectronic device with consideration of thermal coupling between elements of the first hierarchical level which belong to subsystems of the second hierarchical level having different physical natures. Therefore, the most complete model of an optoelectronic device thermal regime consists of a system of multidimensional differential thermal conductivity equations for elements of the first hierarchical level and energy equations for the fluxes of heat transport agents with boundary conditions of the first, second, or third sort, or with matching conditions on boundary surfaces. Realization of such a complete model is difficult even with use of modern computers, since the number of elements at the lowest hierarchical level exceeds several hundreds or thousands. The difficulties which occur are related both to the problem of choosing a solution method and the volume of machine time required, and with the volume of initial data appearing in a full model. Moreover, optoelectronic device construction is performed in accordance with the four-level hierarchy described above. Analysis of the thermal regime at

Precision Mechanics and Optics Institute, Leningrad. Translated from *Inzhenerno-Fizicheskii Zhurnal*, Vol. 54, No. 6, pp. 995-1002, June, 1988. Original article submitted March 18, 1987.